Chemistry–A European Journal
Communication
doi.org/10.1002/chem.202000664

Dioxygen Activation

Exceptional Substrate Diversity in Oxygenation Reactions Catalyzed by a Bis(μ-oxo) Copper Complex

Melanie Paul,[a] Melissa Teubner,[a, b] Benjamin Grimm-Lebsanft,[b] Christiane Golchert,[a] Yannick Meiners,[a] Laura Senft,[c] Kristina Keisers,[a] Patricia Liebhäuser,[a] Thomas Rösener,[a] Florian Biebl,[b] Sören Buchenau,[b] Maria Naumova,[d] Vadim Murzin,[d] Roxanne Krug,[e] Alexander Hoffmann,[a] Jörg Pietruszka,[e, f] Ivana Ivanović-Burmazović,[c] Michael Rübhausen,[b] and Sonja Herres-Pawlis*[a]

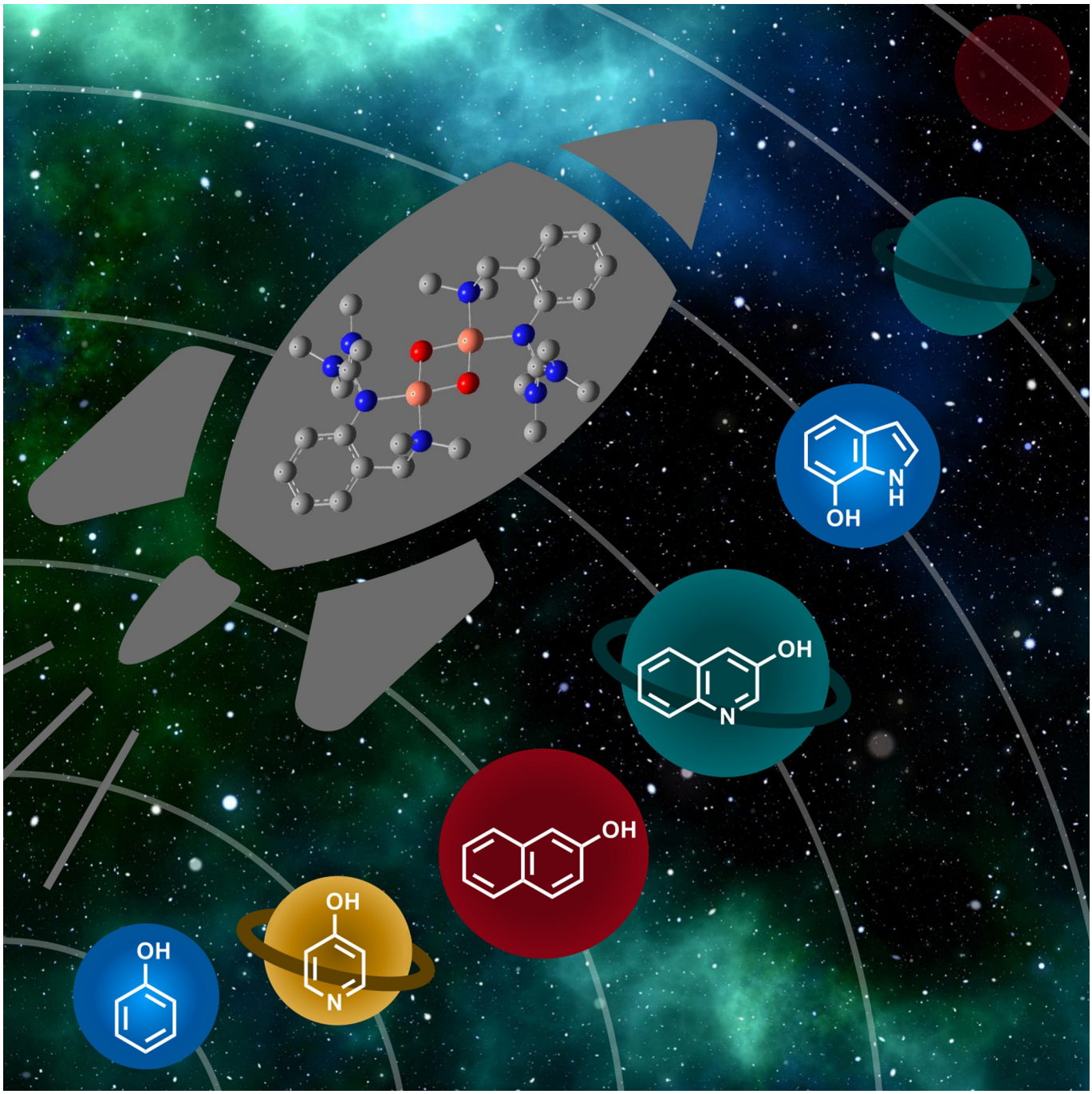

Abstract: The enzyme tyrosinase contains a reactive side-on peroxo dicopper(II) center as catalytically active species in C–H oxygenation reactions. The tyrosinase activity of the isomeric bis(μ-oxo) dicopper(III) form has been discussed controversially. The synthesis of bis(μ-oxo) dicopper(III) species $[Cu_2(\mu\text{-}O)_2(\mathbf{L1})_2](X)_2$ ($[\mathbf{O1}](X)_2$, $X = PF_6^-$, BF_4^-, OTf^-, ClO_4^-), stabilized by the new hybrid guanidine ligand 2-{2-((dimethylamino)methyl)phenyl}-1,1,3,3-tetramethylguanidine (**L1**), and its characterization by UV/Vis, Raman, and XAS spectroscopy, as well as cryo-UHR-ESI mass spectrometry, is described. We highlight selective oxygenation of a plethora of phenolic substrates mediated by $[\mathbf{O1}](PF_6)_2$, which results in mono- and bicyclic quinones and provides an attractive strategy for designing new phenazines. The selectivity is predicted by using the Fukui function, which is hereby introduced into tyrosinase model chemistry. Our bioinspired catalysis harnesses molecular dioxygen for organic transformations and achieves a substrate diversity reaching far beyond the scope of the enzyme.

The use of dioxygen as a readily available oxidizing agent is crucial for many biological and biomimetic oxidation processes, as well as industrial applications.[1] Natural copper enzymes, such as tyrosinase or particulate methane monooxygenase, successfully activate molecular dioxygen.[2] Tyrosinase, in particular, is essential in living organisms catalyzing phenol oxidation in melanin biosynthesis.[3] It converts phenols, for instance, L-tyrosine, via an electrophilic aromatic substitution through its catechol form to the final quinone form.[4] Although structure and reactivity of tyrosinases were studied extensively, many details of the oxidation mechanism are still under debate.[5] Recently, second shell residues at the active site (ca. 5.5–16 Å distance to Cu ions) were considered to direct the reactivity of the enzyme.[2b,6]

For understanding the mechanism of activation and transfer of O_2, synthetic model systems were developed mimicking enzymatic properties. Some well-studied Cu/O_2 species represent $\mu\text{-}\eta^2\text{:}\eta^2$-peroxo Cu^{II} [**P**] and bis(μ-oxo) Cu^{III} [**O**] complexes, which exist in a dynamic equilibrium due to a small isomerization barrier.[2b,7] In many functional tyrosinase systems, **[P]** cores are found,[8] but an increasing number of examples of functional [**O**] species has also been reported.[9] However, only few tyrosinase model systems feature catalytic oxygenation reactivity.[10] Réglier and co-workers presented the first system using the imine–pyridine ligand $BiPh(impy)_2$,[11] followed by Casella and co-workers by using the benzimidazole ligand L66,[12] which both stabilize binuclear Cu catalysts. Later, Tuczek and co-workers reported the mononucleating benzimidazole ligand L^{impy} promoting catalytic conversion of 2,4-di-*tert*-butyl phenol.[13] Over the years, Lumb and co-workers have focused on the chemo- and regioselectivity of tyrosinase-like reactions by using the amine DBED giving rise to several quinones, oxidative coupling, and cyclization products.[14] More complex phenolic substrates were oxygenated by Herres-Pawlis group by using bis(pyrazolyl)methane and guanidine ligands.[15]

Herein, we report the synthesis and characterization of hybrid guanidine-stabilized bis(μ-oxo) complex $[Cu_2(\mu\text{-}O)_2(\mathbf{L1})_2]^{2+}$ ($[\mathbf{O1}]^{2+}$, Scheme 1) along with its high catalytic activity in oxygenation and oxidation reactions of phenolic substrates and subsequent condensation reactions, offering a facile synthetic pathway to new phenazines.

Guanidines feature high basicity and strong N-donor abilities, enabling stabilization of metal ions with high oxidation states.[16] For instance, TMG_3tren is known to stabilize highly reactive Cu^{II} superoxo complexes.[17] By using $[\mathbf{O1}](PF_6)_2$, it is possible to promote selective C–H functionalization of complex phenolic substrates. To the best of our knowledge, no activity of tyrosinases towards complex phenolic substrates has been reported before. Compound $[\mathbf{O1}](PF_6)_2$ highlights a beneficial interplay of steric and electronic factors of the ligand regarding substrate accessibility of $[Cu_2O_2]$ core leading to a remarkable extension of the substrate scope. Using a variety of phenolic substances allows the synthesis of new quinones. In a consecu-

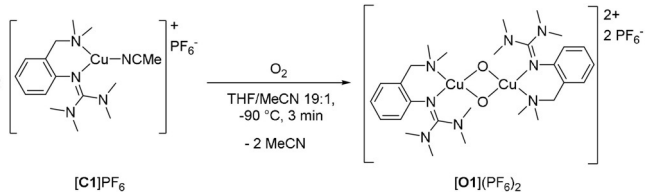

Scheme 1. Synthesis of bis(μ-oxo) species $[\mathbf{O1}](PF_6)_2$.

[a] *M. Paul, M. Teubner, C. Golchert, Y. Meiners, K. Keisers, Dr. P. Liebhäuser, Dr. T. Rösener, Dr. A. Hoffmann, Prof. Dr. S. Herres-Pawlis*
Department of Inorganic Chemistry
RWTH Aachen University, Landoltweg 1, 52074 Aachen (Germany)
E-mail: sonja.herres-pawlis@ac.rwth-aachen.de

[b] *M. Teubner, Dr. B. Grimm-Lebsanft, F. Biebl, S. Buchenau, Prof. Dr. M. Rübhausen*
Department of Physics, University of Hamburg
Luruper Chaussee 149, 22761 Hamburg (Germany)

[c] *L. Senft, Prof. Dr. I. Ivanović-Burmazović*
Department of Chemistry and Pharmacy
Friedrich-Alexander-University of Erlangen-Nürnberg
Egerlandstrasse 1, 91058 Erlangen (Germany)

[d] *Dr. M. Naumova, Dr. V. Murzin*
Deutsches Elektronen-Synchrotron DESY
Notkestrasse 85, 22607 Hamburg (Germany)

[e] *Dr. R. Krug, Prof. Dr. J. Pietruszka*
Institute of Bioorganic Chemistry
Heinrich Heine University Düsseldorf at Forschungszentrum Jülich
52425 Jülich (Germany)

[f] *Prof. Dr. J. Pietruszka*
Institute of Bio- and Geoscience (IBG-1: Biotechnology)
Forschungszentrum Jülich GmbH
52425 Jülich (Germany)

Supporting information and the ORCID identification number(s) for the author(s) of this article can be found under: https://doi.org/10.1002/chem.202000664.

tive reaction, quinones can condense with 1,2-phenylenediamine to phenazines, which feature antibacterial, antimalarial, and antitumor activities, and are used in dyes and pesticides.[18] We targeted to selectively obtain bent phenazines as special benefit of the [**O1**]$(PF_6)_2$-mediated hydroxylation, because the calculation of the Fukui function of the hydroxylation products indicated preferential formation of the corresponding quinone.

Inspired by a propylene-bridged hybrid guanidine ligand system that showed promising phenolase activity,[9k–l] we developed a related ligand system with a more rigid aromatic backbone. Compound 2-{2-((dimethylamino)methyl)phenyl}-1,1,3,3-tetramethylguanidine (**L1**) was synthesized in a three-step reaction and isolated in high yield (see the Supporting Information). Synthesis of the colorless, air- and moisture-sensitive Cu^{I} complex [**C1**]PF_6 was achieved by mixing equimolar amounts of **L1** and $[Cu(MeCN)_4]PF_6$ in acetonitrile at room temperature. Oxygenation of [**C1**]PF_6 in THF at −90 °C led to the formation of the khaki colored species [**O1**]$(PF_6)_2$ (Scheme 1).[19] Compound [**O1**]$(PF_6)_2$ showed ligand-to-metal-charge transfer (LMCT) features at 280 nm ($\varepsilon = 40000\ M^{-1}cm^{-1}$) and 392 nm ($21\,000\ M^{-1}cm^{-1}$) in the UV/Vis spectrum[20] (Figure 1 a), which are characteristic for bis(μ-oxo) dicopper(III) species.[8,21] Similar UV/Vis features were obtained by using different weakly coordinating anions (BF_4^-, ClO_4^-, OTf^-; Figure S17 and Table S3 in the Supporting Information). Incorporated O_2 of [**O1**]$(PF_6)_2$ was resistant to cycles of evacuation and purging with N_2. Laser excitation at 420 nm led to a resonance Raman spectrum with a characteristic vibration at 620 cm^{-1}, which was attributed to the symmetrical Cu_2O_2 core expansion (breathing mode), thus evidencing the formation of a bis(μ-oxo) species (Figure 1 b). $^{16}O_2/^{18}O_2$ isotope exchange measurements in THF exhibited a shift to 591 cm^{-1}, which is in good agreement with theoretical calculations (Table S13 in the Supporting Information). The signal at 530 cm^{-1} is caused by the N(amine)–Cu vibration.

Theoretical studies on [**O1**]$(PF_6)_2$ were performed to investigate geometry and Raman features (Figure 2). The calculations showed that the **O** species is favored by 10 kcal mol^{-1} over the **P** species (Table S11 in the Supporting Information). Key bond lengths around the Cu atoms were determined by Cu K-edge EXAFS (Figure 1 c–d, and section 1.3 in the Supporting Information) and agree well with the theoretical model. Moreover, the edge position is in accordance with the assignment as Cu^{III}. For quantification of the formation of [**O1**]$(PF_6)_2$, spectrophotometric back titration of [**O1**]$(PF_6)_2$ was performed by using ferrocene monocarboxylic acid (FcCOOH).[9k,l] Following the decay of the LMCT band at 392 nm, titration of [**O1**]$(PF_6)_2$ with FcCOOH revealed >90% formation of [**O1**]$(PF_6)_2$ (Figures S18 and 19 in the Supporting Information). To elucidate the Cu–O_2 stoichiometry of [**O1**]$(PF_6)_2$, cryo-UHR-ESI mass spectrometry was performed (Figure S20). The isotopic pattern and corresponding *m/z* values are in accordance with the calculated spectrum of the monocationic species [**O1**]$(PF_6)^+$ with a 2:1 Cu-O_2 ratio.

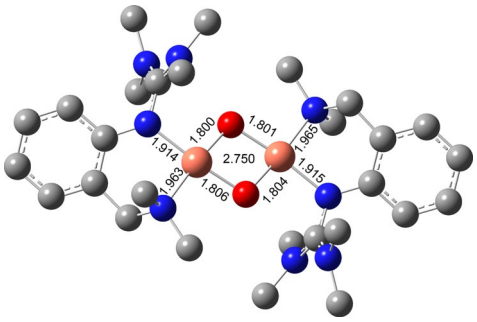

Figure 2. DFT model of $[\mathbf{O1}]^{2+}$ (TPSSh/def2-TZVP, THF-PCM), selected bond lengths [Å] and Cu···Cu vector [Å].

Thermal decomposition kinetics of [**O1**]$(PF_6)_2$ revealed a first-order decay at low temperatures (Figures S21 and 22 in the Supporting Information). Half-life times of [**O1**]$(PF_6)_2$ in THF of 1 h at −80 °C and five minutes at −74 °C were determined. Thermal decomposition products of [**O1**]$(PF_6)_2$ were identified by crystallization as a dicationic μ-alkoxo-μ-hydroxo copper(II) complex [**H1**]$(PF_6)_2$ with a Cu···Cu distance of 2.953(1) Å (Figure 3). Each copper atom is coordinated in a distorted square-planar fashion. The average Cu–O bond length (1.92 Å) is shorter compared to that in the mixed phenolato hydroxo-bridged dicopper(II) species (1.96 Å) reported by Karlin and coworkers.[22] Concomitant formation of yellow blocks was observed, which contain the protonated ligand [(**L1**)H_2]$(PF_6)_2$.

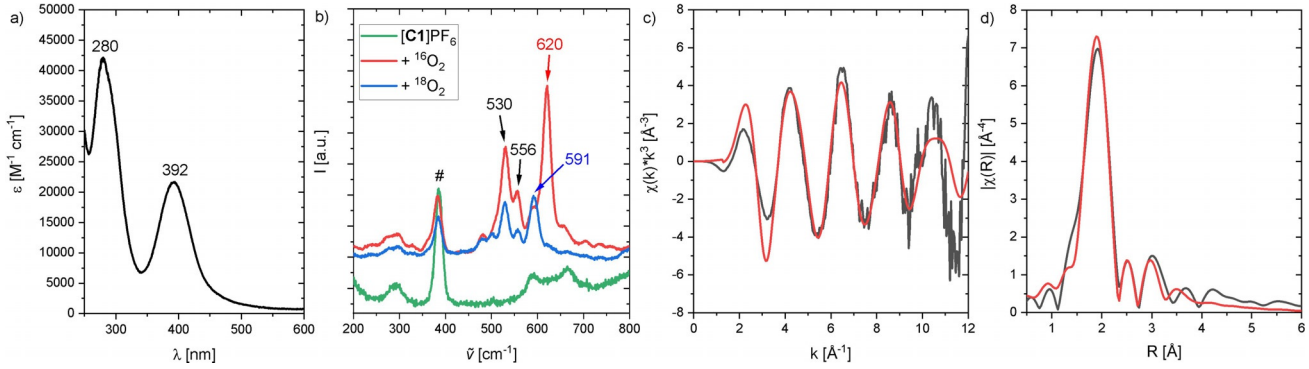

Figure 1. a) UV/Vis spectrum of [**O1**]$(PF_6)_2$ (0.5 mM) in THF at −90 °C; b) resonance Raman spectra of [**O1**]$(PF_6)_2$ in THF with excitation at 420 nm (blue: $^{18}O_2$, red: $^{16}O_2$, green: [**C1**]PF_6, #: solvent); c) k^3-weighted Cu K-edge EXAFS of [**O1**]$(PF_6)_2$ (black: experimental, red: calculated fit); and d) phase-corrected Cu-K-edge Fourier transform of EXAFS of [**O1**]$(PF_6)_2$ (black: experimental, red: calculated fit).

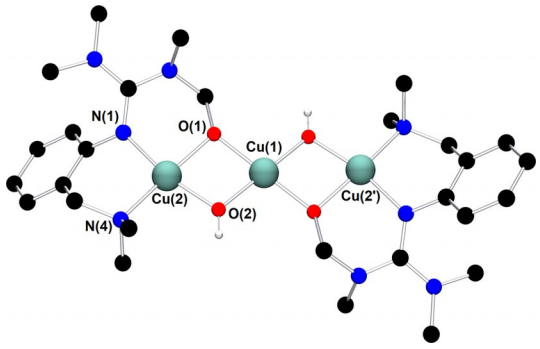

Figure 3. Molecular structure of $[\mathbf{H1}]^{2+}$ in crystals of $[\mathbf{H1}](PF_6)_2$. H atoms, except for the H atom of μ-OH groups, counterions, and solvent molecules are omitted for clarity. Selected interatomic distances [Å] and angles [°]: Cu(1)–O(1) 1.912(2), Cu(1)–O(2) 1.893(2), Cu(2)–O(1) 1.923(2), Cu(2)–O(2) 1.932(2), Cu(1)···Cu(2) 2.953(1), Cu(2)–N(1) 1.986(2), Cu(2)–N(4) 2.019(3); N(1)-Cu(2)-N(4) 94.9(1), O(1)-Cu(2)-O(2) 76.8(1), Cu(2)-O(1)-Cu(1) 100.7(1), Cu(2)-Cu(1)-Cu(2′) 180.0.

Bis(μ-hydroxo) species are commonly observed as decay products[9,18a] and often resulted from intramolecular hydroxylation of C–H bonds in α- or β-position of N-donor groups.[23] Interestingly, $[\mathbf{H1}]^{2+}$ is the first example of a trinuclear μ-alkoxo-μ-hydroxo copper(II) complex cation. Only few examples of alkoxo-hydroxo copper(II) species have been reported to date.[7b,23] Mechanistic studies on intramolecular hydroxylation of the supporting ligand upon warming of the bis(μ-oxo) species were proposed by Itoh, Tolman and co-workers stating a mixed alkoxo-hydroxo copper(II) complex as intermediate species to form thermodynamically stable bis(μ-hydroxo) and bis(μ-alkoxo) complexes.[23a,24] In case of $[\mathbf{H1}]^{2+}$, the chemoselective attack of the equatorially located methyl groups of the guanidine moiety over the axially disposed aminomethyl groups is favored due to geometric constraints, similar to observations made by Tolman and co-workers.[23c,25]

Aiming to expand the commonly used substrate scope of simple phenols, catalytic hydroxylation activity of $[\mathbf{O1}](PF_6)_2$ was evaluated towards a variety of challenging phenolic substrates, including phenols, pyridinols, naphthols, quinolinols, and indolols (Table 1 and section 2.6 in the Supporting Information), quinones and phenazines of which are biologically relevant and difficult to synthesize. We report the hydroxylation of a multitude of these substrates by $[\mathbf{O1}](PF_6)_2$ along with transformation of the quinone into a phenazine. Remarkably that until now, catalytic conversion of phenols was mostly reported for side-on peroxo copper complexes as catalytically active species.[11–13,15] Oxygenation reactions were performed following a protocol established by Bulkowski and modified by Tuczek and co-workers by using 25 equivalents of substrate and 50 equivalents of NEt_3 (Table 1, Reaction (a)).[13a,26] Reaction (a) was monitored by UV/Vis spectroscopy at −90 °C for one hour as optical spectra remained constant after that time. Reactive quinones were subsequently converted in a one-pot reaction into their corresponding phenazines at room temperature by using 1,2-phenylenediamine (Table 1, Reaction (b)).

When simple phenols were used, $[\mathbf{O1}](PF_6)_2$ showed, besides the expected hydroxylation activity, also C–O coupling chemistry (Table S8 in the Supporting Information, entries 1–4). UV/Vis spectra showed a low intensity absorption band at 510 and 530 nm (Figures S39 and 40 in the Supporting Information).

Table 1. Catalytic oxygenation of phenolic substrates[a] and subsequent condensation of the quinone by using 1,2-phenylenediamine.[b]

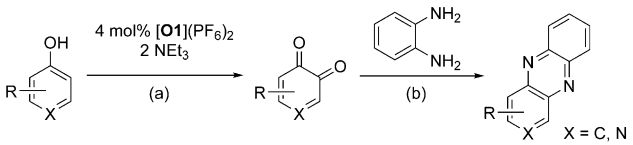

Entry	Substrate	Conv. [%]	Product (quinone/phenazine)		Yield[c] [%]	TON[d]
1	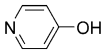	>99		(**Q1**)	[e]	[f]
2	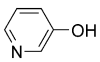	>99		(**Q1**)	[e]	[f]
3		80	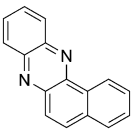	(**P1**)	22	11
4	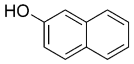	89		(**P1**)	31	16
5	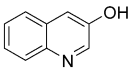	95	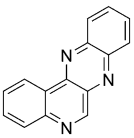	(**P2**)	32	16
6		87		(**P2**)	21	11
7	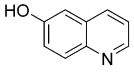	>99	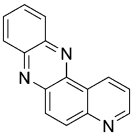	(**P3**)	30	15
8		28	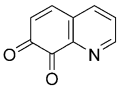	(**Q2**)	–	14[g]
9	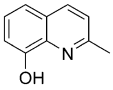	24	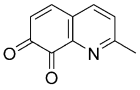	(**Q3**)	–	12[g]
10	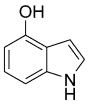	81	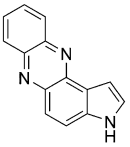	(**P4**)	19	10
11	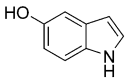	88		(**P4**)	26	13
12	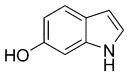	92	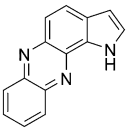	(**P5**)	27	14
13	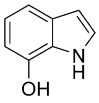	84		(**P5**)	31	16

[a] Conditions: THF, −90 °C, 1 h. [b] Conditions: THF, −90 °C, then rt, overnight. [c] Isolated yield after column chromatography. [d] Based on isolated yield in correlation with conc. of $[\mathbf{O1}](PF_6)_2$. [e] Quinone too reactive to be isolated. [f] No extinction coefficient of the quinone reported. [g] Determined after reaction (a) by UV/Vis spectra and based on conc. of $[\mathbf{O1}](PF_6)_2$.

EPR measurements revealed the hyperfine splitting pattern typical for a radical-free, metal-centered Cu^{II} species, ruling out the formation of a semiquinone species (Figure S41).[27]

An interesting substrate for the catalytic oxygenation is 8-quinolinol.[15,28] Although 7,8-quinolinedione (**Q2**) was formed with 14 turnovers (entry 8), methyl substitution in 2-position resulted in a TON of 12 (**Q3**, entry 9). However, formation of the respective phenazine was observed in neither case (Figures S50 and 51 in the Supporting Information), presumably due to the smaller Fukui function $f+$ at the corresponding C atoms of **Q2** and **Q3** (Table S15). Conversion of other quinolinols was not reported before in Cu/O_2 chemistry. Compounds 3- and 4-quinolinol were transformed into their quinone (absorption band at 370 nm, Figures S47 and 48 in the Supporting Information) and isolated as quinolino[3,4-b]quinoxaline (**P2**; entries 5–6). 6-Quinolinol was oxidized into 5,6-quinolinedione (entry 7), which showed absorption bands at 325, 340, and 370 nm (Figure S49). Pyrido[3,2-a]phenazine (**P3**) was isolated in 15 turnovers after column chromatography and sublimation, and crystallized from DMSO (see the Supporting Information).

In contrast to reactions with phenols and 8-quinolinol, no conversion of pyridinols has been reported to date. When 3- and 4-pyridinol (entries 1–2) were used, an intense absorption band at 375 nm, similar to that in 3- and 4-quinolinol, was observed in both cases within less than one minute (Figures S42 and 43 in the Supporting Information), indicating formation of 3,4-pyridoquinone (**Q1**). A fast drop in intensity illustrates high reactivity of the quinone even at low temperatures, leading to C–O coupled dimers (see the Supporting Information).[29] Theoretical studies revealed lesser stability of 3,4-pyridoquinone compared to its most stable 2,5-isomer.[30] However, no other study exists that reports on pyridoquinones.

Naphthoquinones are accessible from 1- and 2-naphthol in the presence of an oxidizing agent.[31] Both naphthols were converted via [**O1**]$(PF_6)_2$ into the corresponding quinone, which resulted in the formation of benzo[a]phenazine[31c] (**P1**) upon treatment with 1,2-phenylenediamine (entries 3–4, Figures S44 and 45 in the Supporting Information). Compound **P1** was purified by column chromatography and isolated with a TON of 11–16. Consistent with observations made by Krohn and co-workers, no formation of the linear phenazine was observed.[31c] The control experiment by using 1-methyl 2-naphthol (Table S8, entry 7) showed no product formation as was expected (Figure S46), because the 1-position is occupied by the methyl substituent inhibiting the oxygenation process.

Although related bicyclic indolols possess an easily accessible pyrrole ring, C–H functionalization of the phenyl ring remains challenging.[32] When [**O1**]$(PF_6)_2$ was used, 4- and 5-indolol were converted into 4,5-indoledione, which was captured as pyrrolo[3,2-a]phenazine (**P4**) in 10–13 turnovers (entries 10–11, Figures S52 and 53). Similarly, 6- and 7-indolol (Figures S54 and 55) were transformed into pyrrolo[2,3-a]phenazine (**P5**, TON = 14–16) and crystallized from hexane (entries 12–13). The control experiment revealed no oxygenation activity on 6-indolol in the absence of supporting ligand **L1** (Figure S36), thus evidencing the necessity of the stabilizing ligand system.

The accompanying DFT calculations based on the negative Fukui function were used to determine the location of the electrophilic attack, which are in good agreement with the observed products (for substrates with two product possibilities, see Tables 1 and 2 and section 3.2 in the Supporting Information). The Fukui function describes the electron density in a frontier orbital, in this case f_k^- denotes the initial part for an electrophilic reaction. A large value for f_k^- indicates the preferred site for an electrophilic attack—in this case, the tyrosinase-like hydroxylation. In all cased studied herein, the Fukui function points to the experimentally observed hydroxylation site finally yielding the bent phenazines.

Table 2. Summary of calculated Fukui function [f_k^-] of phenolic substrates with two possible products.

Entry	Substrate	f_k^-	C atom position
1	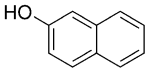	21.14 0.74	1 3
2	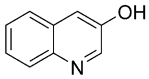	1.38 15.17	2 4
3	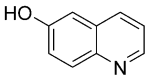	23.93 0.91	5 7
4	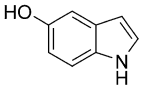	19.93 1.05	4 6
5	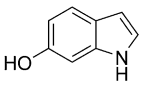	2.03 11.99	5 7

It has to be highlighted that the phenazines **P3**, **P4**, and **P5** are new and fully characterized.[33] Thus, the combination of tyrosinase-like hydroxylation reactivity with the condensation of quinones with diamines allows synthetic access to a multitude of new phenazines.

Although tyrosinase (from *Aspergillus oryzae*) oxidizes phenol quantitatively,[34] the enzyme exhibited no reactivity towards naphthols, quinolinols, and indolols (Table S10 in the Supporting Information). Thus, the bis(μ-oxo) species [**O1**]$(PF_6)_2$ demonstrates an exceptional broad substrate scope to which the enzyme itself gave no access.

In summary, we established the synthesis of the aromatic hybrid guanidine-stabilized bis(μ-oxo) species $[\mathbf{O1}]^{2+}$, which was clearly evidenced by its spectroscopic properties. Compound [**O1**]$(PF_6)_2$ revealed a moderate stability at low temperatures with a distinguished activity towards a large variety of phenolic substrates. DFT calculations enabled a prognosis of the hydroxylation position by Fukui function, which fully agreed with experimental results. The Fukui function was introduced as new predictive tool for Cu/O_2 chemistry. Moreover, our present findings clearly show efficient C–H activation of mono- and bicyclic phenolic substrates, stating an atom-eco-

nomic strategy to design new phenazines. A bioinspired model system, such as [**O1**](PF$_6$)$_2$, indicates tyrosinase-like activity of **O** cores and exceeds evidently the enzymatically limited substrate scope. This study opens the door to future developments on tyrosinase model systems with high relevance to atom-economic oxygen-transfer reactions with synthetic importance.

Acknowledgements

We acknowledge financial support provided by the German Research Foundation (DFG), in framework of Priority Program "Reactive Bubbly Flows" SPP 1740 (HE 5480/10-2, http://www.dfg-spp1740.de/), International Research Training Group SeleCa and further projects (RU 773/8-1). We also acknowledge computing time and support provided by OCuLUS Cluster at PC^2 Paderborn and support at beamline P64 by Marcel Görlitz and Dr. Wolfgang Caliebe.

Conflict of interest

The authors declare no conflict of interest.

Keywords: copper catalysis · dioxygen activation · guanidines · phenazines · tyrosinase

[1] a) A. N. Campbell, S. S. Stahl, *Acc. Chem. Res.* **2012**, *45*, 851 – 863; b) S. D. McCann, S. S. Stahl, *Acc. Chem. Res.* **2015**, *48*, 1756 – 1766.

[2] a) E. I. Solomon, D. E. Heppner, E. M. Johnston, J. W. Ginsbach, J. Cirera, M. Qayyum, M. T. Kieber-Emmons, C. H. Kjaergaard, R. G. Hadt, L. Tian, *Chem. Rev.* **2014**, *114*, 3659 – 3853; b) C. E. Elwell, N. L. Gagnon, B. D. Neisen, D. Dhar, A. D. Spaeth, G. M. Yee, W. B. Tolman, *Chem. Rev.* **2017**, *117*, 2059 – 2107.

[3] a) Y. Matoba, T. Kumagai, A. Yamamoto, H. Yoshitsu, M. Sugiyama, *J. Biol. Chem.* **2006**, *281*, 8981 – 8990; b) A. Bijelic, M. Pretzler, C. Molitor, F. Zekiri, A. Rompel, *Angew. Chem. Int. Ed.* **2015**, *54*, 14677 – 14680; *Angew. Chem.* **2015**, *127*, 14889 – 14893.

[4] a) V. Kahn, N. Ben-Shalom, *Pigment Cell Res.* **1998**, *11*, 24 – 33; b) M. del Mar Garcia-Molina, J. L. Muñoz-Muñoz, F. Garcia-Molina, P. A. García-Ruiz, F. Garcia-Canovas, *J. Agric. Food Chem.* **2012**, *60*, 6447 – 6453.

[5] a) T. A. G. Large, V. Mahadevan, W. Keown, T. D. P. Stack, *Inorg. Chim. Acta* **2019**, *486*, 782 – 792; b) L. Chiang, E. C. Wasinger, Y. Shimazaki, V. Young, T. Storr, T. D. P. Stack, *Inorg. Chim. Acta* **2018**, *481*, 151 – 158; c) D. A. Quist, D. E. Diaz, J. J. Liu, K. D. Karlin, *J. Biol. Inorg. Chem.* **2017**, *22*, 253 – 288.

[6] a) M. Kanteev, M. Goldfeder, A. Fishman, *Protein Sci.* **2015**, *24*, 1360 – 1369; b) B. Deri, M. Kanteev, M. Goldfeder, D. Lecina, V. Guallar, N. Adir, A. Fishman, *Sci. Rep.* **2016**, *6*, 34993; c) A. Singha, A. Rana, A. Dey, *Inorg. Chim. Acta* **2019**, *487*, 63 – 69.

[7] a) C. J. Cramer, B. A. Smith, W. B. Tolman, *J. Am. Chem. Soc.* **1996**, *118*, 11283 – 11287; b) V. Mahadevan, Z. Hou, A. P. Cole, D. E. Root, T. K. Lal, E. I. Solomon, T. D. P. Stack, *J. Am. Chem. Soc.* **1997**, *119*, 11996 – 11997.

[8] P. Liebhäuser, A. Hoffmann, S. Herres-Pawlis in *Reference Module in Chemistry, Molecular Sciences and Chemical Engineering*, https://doi.org/10.1016/B978-0-12-409547-2.11554-9.

[9] a) D. A. Handley, P. B. Hitchcock, T. H. Lee, G. J. Leigh, *Inorg. Chim. Acta* **2001**, *316*, 59 – 64; b) J. Mukherjee, R. Mukherjee, *Dalton Trans.* **2006**, *6*, 1611; c) L. M. Mirica, T. D. P. Stack, *Inorg. Chem.* **2005**, *44*, 2131 – 2133; d) A. Kunishita, M. Kubo, H. Ishimaru, T. Ogura, H. Sugimoto, S. Itoh, *Inorg. Chem.* **2008**, *47*, 12032 – 12039; e) S. Hong, L. M. R. Hill, A. K. Gupta, B. D. Naab, J. B. Gilroy, R. G. Hicks, C. J. Cramer, W. B. Tolman, *Inorg. Chem.* **2009**, *48*, 4514 – 4523; f) M. Taki, S. Teramae, S. Nagatomo, Y. Tachi, T. Kitagawa, S. Itoh, S. Fukuzumi, *J. Am. Chem. Soc.* **2002**, *124*, 6367 – 6377; g) A. P. Cole, V. Mahadevan, L. M. Mirica, X. Ottenwaelder, T. D. P. Stack, *Inorg. Chem.* **2005**, *44*, 7345 – 7364; h) C. Citek, C. T. Lyons, E. C. Wasinger, T. D. P. Stack, *Nat. Chem.* **2012**, *4*, 317 – 322; i) L. Chiang, W. Keown, C. Citek, E. C. Wasinger, T. D. P. Stack, *Angew. Chem. Int. Ed.* **2016**, *55*, 10453 – 10457; *Angew. Chem.* **2016**, *128*, 10609 – 10613; j) C. C. L. McCrory, A. Devadoss, X. Ottenwaelder, R. D. Lowe, T. D. P. Stack, C. E. D. Chidsey, *J. Am. Chem. Soc.* **2011**, *133*, 3696 – 3699; k) S. Herres-Pawlis, P. Verma, R. Haase, P. Kang, C. T. Lyons, E. C. Wasinger, U. Flörke, G. Henkel, T. D. P. Stack, *J. Am. Chem. Soc.* **2009**, *131*, 1154 – 1169; l) S. Herres-Pawlis, R. Haase, P. Verma, A. Hoffmann, P. Kang, T. D. P. Stack, *Eur. J. Inorg. Chem.* **2015**, 5426 – 5436.

[10] J. N. Hamann, B. Herzigkeit, R. Jurgeleit, F. Tuczek, *Coord. Chem. Rev.* **2017**, *334*, 54 – 66.

[11] M. Réglier, C. Jorand, B. Waegell, *J. Chem. Soc. Chem. Commun.* **1990**, 1752 – 1755.

[12] L. Casella, M. Gullotti, R. Radaelli, P. Di Gennaro, *J. Chem. Soc. Chem. Commun.* **1991**, 1611.

[13] a) M. Rolff, J. Schottenheim, G. Peters, F. Tuczek, *Angew. Chem. Int. Ed.* **2010**, *49*, 6438 – 6442; *Angew. Chem.* **2010**, *122*, 6583 – 6587; b) B. Herzigkeit, B. M. Flöser, N. E. Meißner, T. A. Engesser, F. Tuczek, *ChemCatChem* **2018**, *10*, 5402 – 5405; c) J. N. Hamann, F. Tuczek, *Chem. Commun.* **2014**, *50*, 2298 – 2300; d) B. Herzigkeit, B. M. Flöser, T. A. Engesser, C. Näther, F. Tuczek, *Eur. J. Inorg. Chem.* **2018**, 3058 – 3069; e) B. Herzigkeit, R. Jurgeleit, B. M. Flöser, N. E. Meißner, T. A. Engesser, C. Näther, F. Tuczek, *Eur. J. Inorg. Chem.* **2019**, 2258 – 2266; f) J. Schottenheim, C. Gernert, B. Herzigkeit, J. Krahmer, F. Tuczek, *Eur. J. Inorg. Chem.* **2015**, 3501 – 3511.

[14] a) K. V. N. Esguerra, Y. Fall, J. P. Lumb, *Angew. Chem. Int. Ed.* **2014**, *53*, 5877 – 5881; *Angew. Chem.* **2014**, *126*, 5987 – 5991; b) M. S. Askari, L. A. Rodríguez-Solano, A. Proppe, B. McAllister, J.-P. Lumb, X. Ottenwaelder, *Dalton Trans.* **2015**, *44*, 12094 – 12097; c) Z. Huang, O. Kwon, H. Huang, A. Fadli, X. Marat, M. Moreau, J.-P. Lumb, *Angew. Chem. Int. Ed.* **2018**, *57*, 11963 – 11967; *Angew. Chem.* **2018**, *130*, 12139 – 12143.

[15] a) A. Hoffmann, C. Citek, S. Binder, A. Goos, M. Rübhausen, O. Troeppner, I. Ivanović-Burmazović, E. C. Wasinger, T. D. P. Stack, S. Herres-Pawlis, *Angew. Chem. Int. Ed.* **2013**, *52*, 5398 – 5401; *Angew. Chem.* **2013**, *125*, 5508 – 5512; b) F. Strassl, A. Hoffmann, B. Grimm-Lebsanft, D. Rukser, F. Biebl, M. Tran, F. Metz, M. Rübhausen, S. Herres-Pawlis, *Inorganics* **2018**, *6*, 114.

[16] a) J. Stanek, T. Rösener, A. Metz, J. Mannsperger, A. Hoffmann, S. Herres-Pawlis, *Top. Heterocycl. Chem.* **2015**, *51*, 95 – 164; b) S. Herres-Pawlis, S. Binder, A. Eich, R. Haase, B. Schulz, G. Wellenreuther, G. Henkel, M. Rübhausen, W. Meyer-Klaucke, *Chem. Eur. J.* **2009**, *15*, 8678 – 8682; c) A. Hoffmann, M. Wern, T. Hoppe, M. Witte, R. Haase, P. Liebhäuser, J. Glatthaar, S. Herres-Pawlis, S. Schindler, *Eur. J. Inorg. Chem.* **2016**, 4744 – 4751; d) D. Schurr, F. Strassl, P. Liebhäuser, G. Rinke, R. Dittmeyer, S. Herres-Pawlis, *React. Chem. Eng.* **2016**, *1*, 485 – 493.

[17] a) M. Schatz, V. Raab, S. P. Foxon, G. Brehm, S. Schneider, M. Reiher, M. C. Holthausen, J. Sundermeyer, S. Schindler, *Angew. Chem. Int. Ed.* **2004**, *43*, 4360 – 4363; *Angew. Chem.* **2004**, *116*, 4460 – 4464; b) D. Maiti, D.-H. Lee, K. Gaoutchenova, C. Würtele, M. C. Holthausen, A. A. Narducci Sarjeant, J. Sundermeyer, S. Schindler, K. D. Karlin, *Angew. Chem. Int. Ed.* **2008**, *47*, 82 – 85; *Angew. Chem.* **2008**, *120*, 88 – 91.

[18] a) B. Cross, C. L. Dunn, D. H. Payne, J. D. Tipton, *J. Sci. Food Agric.* **1969**, *20*, 340 – 344; b) N. Guttenberger, W. Blankenfeldt, R. Breinbauer, *Bioorg. Med. Chem.* **2017**, *25*, 6149 – 6166; c) V. F. de Andrade-Neto, M. O. F. Goulart, J. F. da Silva Filho, M. J. da Silva, M. do C. F. R. Pinto, A. V. Pinto, M. G. Zalis, L. H. Carvalho, A. U. Krettli, *Bioorg. Med. Chem. Lett.* **2004**, *14*, 1145 – 1149; d) A. K. Jana, *J. Photochem. Photobiol. A* **2000**, *132*, 1 – 17; e) A. V. Gulevskaya, *Eur. J. Org. Chem.* **2016**, 4207 – 4214; f) F. B. Mortzfeld, J. Pietruszka, I. R. Baxendale, *Eur. J. Org. Chem.* **2019**, 5424 – 5433; g) J. N. Hamann, M. Rolff, F. Tuczek, *Dalton Trans.* **2015**, *44*, 3251 – 3258; h) A. Chaudhary, J. M. Khurana, *Res. Chem. Intermed.* **2018**, *44*, 1045 – 1083; i) Y. Xiao, W. Hu, S. Sun, J.-T. Yu, J. Cheng, *Synlett* **2019**, *30*, 2113 – 2122; j) S. Banerjee, *Arkivoc* **2016**, 82 – 110; k) M. Bilal, S. Guo, H. M. N. Iqbal, H. Hu, W. Wang, X. Zhang, *World J. Microbiol. Biotechnol.* **2017**, *33*, 191; l) A. Cimmino, A. Evidente, V. Mathieu, A. Andolfi, F. Lefranc, A. Kornienko, R. Kiss, *Nat. Prod. Rep.* **2012**, *29*, 487 – 501.

[19] Formation of [**O1**](PF$_6$)$_2$ at −80 °C led to smaller extinction at 392 nm (20000 $M^{-1}cm^{-1}$, −5%) in the UV/Vis spectrum compared to the forma-

tion at −90 °C. Formation of [**O1**](PF$_6$)$_2$ at −74 °C led to a significant loss in quantity (16000 м$^{-1}$cm^{-1}, −24%) (see Supporting Information).
[20] High extinction of [**O1**](PF$_6$)$_2$ at 280 nm is caused by overlapping in-plane π_{o^*} to d_{xy} CT transition and π to π^* transition of the aromatic ligand backbone.
[21] L. M. Mirica, X. Ottenwaelder, T. D. P. Stack, *Chem. Rev.* **2004**, *104*, 1013–1045.
[22] K. D. Karlin, J. C. Hayes, Y. Gultneh, R. W. Cruse, J. W. McKown, J. P. Hutchinson, J. Zubieta, *J. Am. Chem. Soc.* **1984**, *106*, 2121–2128.
[23] a) S. Itoh, M. Taki, H. Nakao, P. L. Holland, W. B. Tolman, L. Que, Jr., S. Fukuzumi, *Angew. Chem. Int. Ed.* **2000**, *39*, 398–400; *Angew. Chem.* **2000**, *112*, 409–411; b) H. Arii, Y. Saito, S. Nagatomo, T. Kitagawa, Y. Funahashi, K. Jitsukawa, H. Masuda, *Chem. Lett.* **2003**, *32*, 156–157; c) S. Mahapatra, J. A. Halfen, W. B. Tolman, *J. Am. Chem. Soc.* **1996**, *118*, 11575–11586; d) M. Enomoto, T. Aida, *J. Am. Chem. Soc.* **1999**, *121*, 874–875.
[24] a) E. A. Lewis, W. B. Tolman, *Chem. Rev.* **2004**, *104*, 1047–1076; b) J. A. Halfen, V. G. Young, W. B. Tolman, *Inorg. Chem.* **1998**, *37*, 2102–2103; c) S. Itoh, H. Nakao, L. M. Berreau, T. Kondo, M. Komatsu, S. Fukuzumi, *J. Am. Chem. Soc.* **1998**, *120*, 2890–2899.
[25] S. Mahapatra, S. Kaderli, A. Llobet, Y.-M. Neuhold, T. Palanché, J. A. Halfen, V. G. Young, T. A. Kaden, L. Que, A. D. Zuberbühler, W. B. Tolman, *Inorg. Chem.* **1997**, *36*, 6343–6356.
[26] J. E. Bulkowski, *Binucleating Ligand–Metal Complexes as Oxidation Catalysts*, US Patent 4,545,937, **1985**.
[27] P. Verma, J. Weir, L. Mirica, T. D. P. Stack, *Inorg. Chem.* **2011**, *50*, 9816–9825.
[28] a) P. Liebhäuser, K. Keisers, A. Hoffmann, T. Schnappinger, I. Sommer, A. Thoma, C. Wilfer, R. Schoch, K. Stührenberg, M. Bauer, M. Dürr, I. Ivanović-Burmazović, S. Herres-Pawlis, *Chem. Eur. J.* **2017**, *23*, 12171–12183; b) C. Wilfer, P. Liebhäuser, A. Hoffmann, H. Erdmann, O. Grossmann, L. Runtsch, E. Paffenholz, R. Schepper, R. Dick, M. Bauer, M. Dürr, I. Ivanovic-Burmazovic, S. Herres-Pawlis, *Chem. Eur. J.* **2015**, *21*, 17639–17649.
[29] Turnovers could not be determined, because no extinction coefficient of the quinone is reported elsewhere in the literature.
[30] I. Yavari, Z. Nader, *Dye. Pigment.* **2007**, *75*, 474–478.
[31] a) A. K. Mishra, J. N. Moorthy, *J. Org. Chem.* **2016**, *81*, 6472–6480; b) A. Wu, Y. Duan, D. Xu, T. M. Penning, R. G. Harvey, *Tetrahedron* **2010**, *66*, 2111–2118; c) H. Hussain, S. Specht, S. R. Sarite, M. Saeftel, A. Hoerauf, B. Schulz, K. Krohn, *J. Med. Chem.* **2011**, *54*, 4913–4917.
[32] J. A. Leitch, Y. Bhonoah, C. G. Frost, *ACS Catal.* **2017**, *7*, 5618–5627.
[33] Furthermore, we report NMR, IR, and MS analytical data for **P2**. Another synthetic route and elemental analysis data have been published previously: L. R. Morgan, R. J. Schunior, J. H. Boyer, *J. Org. Chem.* **1963**, *28*, 260–261.
[34] a) R. Krug, D. Schröder, J. Gebauer, S. Suljić, Y. Morimoto, N. Fujieda, S. Itoh, J. Pietruszka, *Eur. J. Org. Chem.* **2018**, 1789–1796; b) L. Penttinen, C. Rutanen, J. Jänis, J. Rouvinen, N. Hakulinen, *ChemBioChem* **2018**, *19*, 2348–2352.

Manuscript received: February 6, 2020
Revised manuscript received: February 26, 2020
Accepted manuscript online: February 27, 2020
Version of record online: May 19, 2020